JPE 7-2-9

Robust Tracking Control Based on Intelligent Sliding-Mode Model-Following Position Controllers for PMSM Servo Drives

Fayez F. M. El-Sousy †

† Department of Power Electronics & Energy Conversion, Electronics Research Institute (ERI), Dokki, Cairo, Egypt

ABSTRACT

In this paper, an intelligent sliding-mode position controller (ISMC) for achieving favorable decoupling control and high precision position tracking performance of permanent-magnet synchronous motor (PMSM) servo drives is proposed. The intelligent position controller consists of a sliding-mode position controller (SMC) in the position feed-back loop in addition to an on-line trained fuzzy-neural-network model-following controller (FNNMFC) in the feedforward loop. The intelligent position controller combines the merits of the SMC with robust characteristics and the FNNMFC with on-line learning ability for periodic command tracking of a PMSM servo drive. The theoretical analyses of the sliding-mode position controller are described with a second order switching surface (PID) which is insensitive to parameter uncertainties and external load disturbances. To realize high dynamic performance in disturbance rejection and tracking characteristics, an on-line trained FNNMFC is proposed. The connective weights and membership functions of the FNNMFC are trained on-line according to the model-following error between the outputs of the reference model and the PMSM servo drive system. The FNNMFC generates an adaptive control signal which is added to the SMC output to attain robust model-following characteristics under different operating conditions regardless of parameter uncertainties and load disturbances. A computer simulation is developed to demonstrate the effectiveness of the proposed intelligent sliding mode position controller. The results confirm that the proposed ISMC grants robust performance and precise response to the reference model regardless of load disturbances and PMSM parameter uncertainties.

Keywords: PMSM Servo Drives, Field-Oriented Control, Sliding-Mode Control, Fuzzy-Neural-Network Control, Intelligent Model Following Control

1. Introduction

In recent years, advancements in magnetic materials, semiconductor power devices and control theories have made the permanent-magnet synchronous motor (PMSM) drives play a vitally important role in motion-control applications. PMSMs are widely used in high-performance servo applications such as industrial robots and machine tools because of their compact size, high-power density, high air-gap flux density, high-torque/inertia ratio, high torque capability, high efficiency and free maintenance. When compared with an induction motor servo drive, the PMSM has many advantages. For instance, it has higher

Manuscript received February. 2, 2007; revised March 8, 2007
†Corresponding Author: fayez@eri.sci.eg
Tel: +202-310554, Fax: +202-3351631, ERI
Dept. of Power Electronics & Energy Conversion, ERI

efficiency, resulting from the absence of rotor losses and lower no-load current below the rated speed. Utilizing the vector control technique or field-oriented control (FOC) technique simplifies the dynamic model of the PMSM and control scheme. Also, the vector control technique is employed in order to obtain high torque capability of the PMSM drive through the decoupling control of *d-q* axes stator currents in the rotor reference frame. For a PMSM, the PM provides the flux linkage, λ_m. By keeping *d*-axis current, $i_{ds}^r = 0$, the PMSM torque may vary linearly with the *q*-axis current component, i_{qs}^r, and the maximum torque per ampere is achieved which is similar to the control of a separately excited DC motor [1]-[4].

In recent years, the variable structure control (VSC) with sliding-mode or sliding-mode control (SMC) has received much attention in the control of PMSM servo drives because the SMC can offer beneficial properties such as insensitivity to parameter variations, external load disturbance rejection and fast dynamic response [5]. SMC is one of the effective nonlinear robust control approaches since it provides system dynamics with an invariance property to uncertainties once the system dynamics are controlled in the sliding mode. The attribute of the SMC system is that the controller is switched between two distinct control structures, reaching phase and sliding phase. The first step of SMC design is to select a sliding surface that models the desired closed-loop performance in state variable space. The controller is designed such that the system state trajectories are forced toward the sliding surface. The system state trajectory in the period of time before reaching the sliding surface is called the reaching phase. Once the system trajectory reaches the sliding surface, the sliding mode occurs and the system slides along it to the origin. The insensitivity of the controlled system to uncertainties exists in the sliding phase, but not during the reaching phase. Thus, the system dynamic in the reaching phase is still influenced by uncertainties. To keep robustness in the whole sliding-mode control system, several researchers have focused on eliminating the effect of the reaching phase [6]-[9]. A sliding curve, chosen as close as possible to the time-optimal trajectory, was proposed in [6]-[9] to keep robustness from the initial point to final point. However, the system dynamics are still subject to uncertainties.

Intelligent control techniques in much research have been developed to improve the performance of the PMSM servo drives and to deal with the nonlinearities and uncertainties of the dynamic model of the PMSM using fuzzy logic, neural network and/or the hybrid of them. It is well known that the neural networks need to be trained and their training is time consuming. High convergence accuracy and a high convergence rate are desirable for the training of the neural network. The most popular training algorithm for a multi-layer neural network is the back propagation [10]-[11]. The concept of incorporating fuzzy logic into a neural network has grown into a popular research topic. In contrast to the pure neural network or fuzzy system, the fuzzy neural network (FNN) possesses both their advantages; it combines the capability of fuzzy reasoning in handling uncertain information and the capability of artificial neural networks in learning from the process. However, the adaptive control schemes that incorporate the techniques of FNNs have also grown rapidly [12]-[17].

The aim of this paper is to design a proposed intelligent sliding-mode position controller for a PMSM servo drive system. The intelligent position controller consists of a sliding-mode position controller in the position feed-back loop in addition to an on-line trained fuzzy-neural-network model-following controller (FNNMFC) in the feedforward loop. In this paper, first, a sliding-mode position controller is applied to the control of the rotor position of a PMSM servo drive. In the sliding-mode control, when the sliding mode occurs, the servo drive system dynamic behaves as a robust state feedback control system. At this point, a proposed on-line trained FNNMFC system is designed in addition to the SMC to improve the dynamic performance and to preserve favorable model-following characteristics under various operating conditions of the servo drive system. In the proposed on-line trained FNNMFC, the error between the reference model and the PMSM servo drive system output is used to train the connective weights and membership functions of the FNNMFC. The output of the FNNMFC is added to the sliding-mode position controller output to compensate for the error between the reference model and the PMSM servo drive system output under parameter variations uncertainties and external load

disturbances. The dynamic performance of the PMSM servo drive system has been studied under load changes and parameter uncertainties. The simulation results are given to demonstrate the effectiveness of the proposed controllers. The proposed servo drive system is shown in Fig. 1.

2. Field-oriented Control and Dynamics of the PMSM Servo Drive System

The mathematical modeling of the PMSM in the synchronously rotating rotor reference frames can be derived as follows [1-2, 10]. The stator voltage equations in the d^r-q^r synchronously rotating rotor reference frame can be carried out as follows:

$$V_{qs}^r = R_s i_{qs}^r + L_{ss}\frac{d}{dt}i_{qs}^r + \omega_r L_{ss} i_{ds}^r + \omega_r \lambda_m' \tag{1}$$

$$V_{ds}^r = R_s i_{ds}^r + L_{ss}\frac{d}{dt}i_{ds}^r - \omega_r L_{ss} i_{qs}^r \tag{2}$$

The electromagnetic torque can be expressed as:

$$T_e = \frac{3}{2}\cdot\frac{P}{2}\cdot\lambda_m i_{qs}^r \tag{3}$$

$$T_e = J_m\left(\frac{2}{P}\right)\frac{d^2\theta_r}{dt^2} + \beta_m\left(\frac{2}{P}\right)\frac{d\theta_r}{dt} + T_L \tag{4}$$

Where V_{qs}, V_{ds}, i_{qs} and i_{ds} are the stator voltages and currents respectively. R_s and L_{ss} are the resistance and self inductance of the stator. θ_r, J_m , β_m and P are the rotor position, electrical rotor speed, effective inertia, friction coefficient and the number of poles of the motor respectively. T_e, T_L, and τ_s are the electromagnetic torque, the load torque and the stator time constant of the motor respectively. λ_m, e_{qs} and e_{ds} are the flux linkage, back *emfs* in the *d-q* axes rotor reference frame respectively.

The PMSM used in this drive system is a three-phase type, 1 hp, 4 poles, 208 V, 60 Hz, 1800 rpm, voltage constant: 0.314 v.s/rad, R_s=1.5 Ω, L_{ss}=0.05 H, J_m=0.003 kg.m^2 and β_m=0.0009 N.m/rad/sec. For the position control system, the PMSM is operated as a motor and is driven by a current-regulated pulse width modulation (CRPWM) inverter. With the implementation of field-oriented control, the PMSM servo drive can be simplified to a control system block diagram as shown in Fig. 2 [10], in which the electromagnetic torque can be simplified as:

$$T_e = K_t i_{qs}^{r*} \tag{5}$$

With $K_t = (3/2).(P/2).\lambda_m$ and K_t is the torque constant.

The mechanical equation of the PMSM servo drive can be represented as:

$$T_e = J_m(2/P)\ddot{\theta}_r(t) + \beta_m(2/P)\dot{\theta}_r(t) + T_L \tag{6}$$

By substituting (5) into (6), the mechanical dynamics of the PMSM servo drive system can be simplified as:

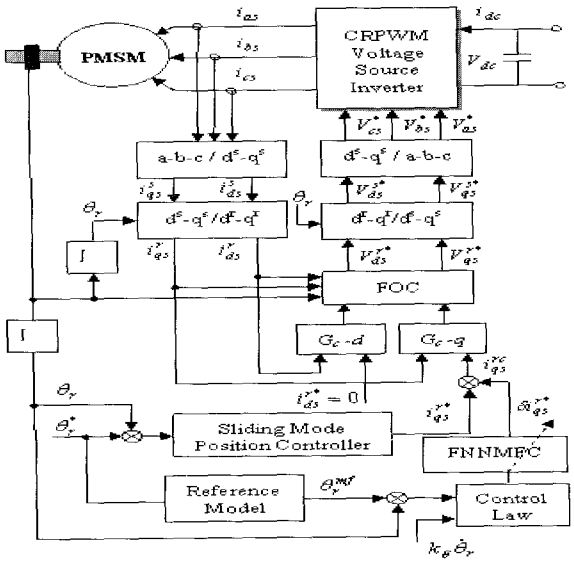

Fig. 1 The block schematic diagram of a FOC-PMSM servo drive system

$$\ddot{\theta}_r = -\frac{\beta_m}{J_m}\cdot\frac{P}{2}\dot{\theta}_r + \frac{K_t}{J_m(P/2)}\cdot i_{qs}^{r*} - \frac{P}{2}\cdot\frac{1}{J_m}\cdot T_L \tag{7}$$

$$\ddot{\theta}_r = A_m\dot{\theta}_r + B_m U(t) + D_m T_L \tag{8}$$

Where,

$$A_m = -\frac{\beta_m}{J_m}\cdot\frac{P}{2}, B_m = \frac{K_t}{J_m(P/2)}, D_m = -\frac{P}{2}\cdot\frac{1}{J_m}\cdot T_L, U(t) = i_{qs}^{r*}(t)$$

is the control effort.

In [11], a two-degrees-of-freedom integral plus proportional & rate feedback (2DOF I-PD) position controller is designed to stabilize the position control loop. The gains of the 2DOF I-PD position controller have been determined using the ITAE performance index response method to obtain the desired control performance in the nominal condition of command tracking. The 2DOF I-PD position controller parameters and the reference model are given by:

$$K_p^{\theta} = \frac{1}{c_o \bar{K}}(3.4\omega_n^4 - \tau_1 \omega_n^5) \tag{9}$$

$$K_i^{\theta} = \frac{\omega_n^5}{c_o \bar{K}} \tag{10}$$

$$K_d^{\theta} = \frac{1}{c_o \tau_1 \bar{K}}(5\omega_n^2 - c_1) \tag{11}$$

$$G_{rm}^{\theta}(s) = \frac{K^{\theta} d_o (1+\tau_1^{\theta} s)}{d_5 s^5 + d_4 s^4 + d_3 s^3 + d_2 s^2 + d_1 s^1 + d_o} \tag{12}$$

3. Robust intelligent sliding-mode position control system

In this section, an intelligent sliding-mode position controller is proposed to control the position of the PMSM servo drive system. The intelligent sliding-mode position control system for the PMSM servo drive system is shown in Fig. 2, in which the reference model is used as the closed loop transfer function of the servo drive system with the 2DOF I-PD position controller. The parameters of the position controller are chosen according to prescribed time-domain specifications. Although the desired tracking and regulation performance can be realized using the 2DOF I-PD position controller, the control performance of the servo drive system is still sensitive to the uncertainties such as mechanical parameter uncertainty, electrical parameter uncertainty and unstructured uncertainty due to non-ideal field orientation in the transient state. To solve this problem, an intelligent sliding-mode position controller is proposed to increase the robustness of the FOC-PMSM servo drive system. The proposed intelligent position controller combines the SMC and the FNNMFC. The adaptive control law is designed as:

$$i_{qs}^{rc}(t) = U_{SMC}(t) + U_{FNNMFC}(t) = i_{qs}^{r*}(t) + \delta i_{qs}^{r*}(t) \tag{13}$$

The q-axis current command, i_{qs}^{r*}, is generated from the sliding-mode position controller, δi_{qs}^{r*} is the adaptive control signal generated from the proposed FNNMFC to automatically compensate the performance degradation due to load disturbances and PMSM parameter uncertainties. The inputs to the sliding mode controller are the position error, e_{θ}, and the rotor speed ω_r to construct the sliding surface $S(t)$ and the sliding-mode control law to get the q-axis current command, $U_{SMC} = i_{qs}^{r*}$. While the inputs to the FNNMFC are the error between the reference model and actual rotor position, e_{θ}^{mf}, and the rate of change of the rotor position (speed), $K_{\theta}\dot{\theta}_r$. Those signals are used to train the

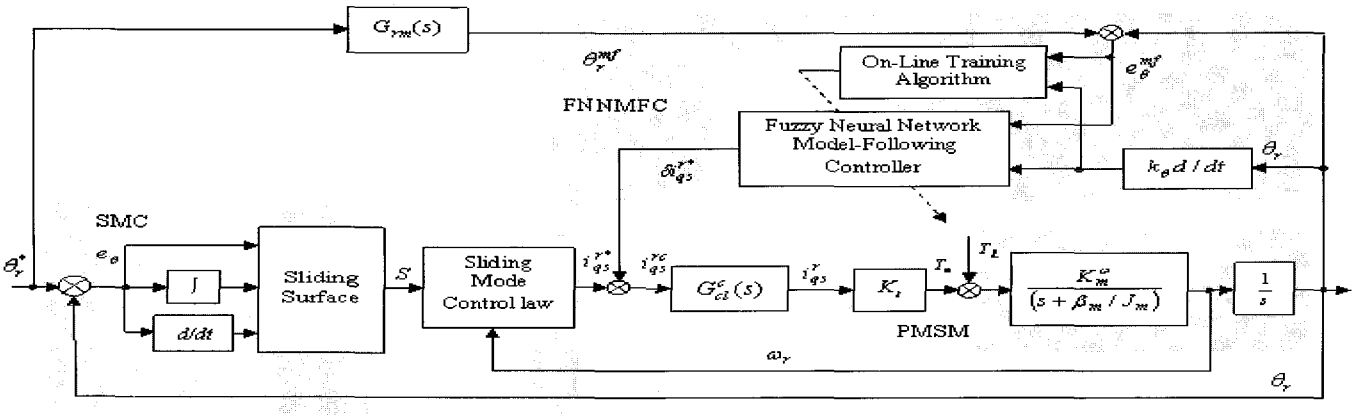

Fig. 2 Structure of the proposed intelligent sliding-mode control (ISMC) for a FOC-PMSM servo drive system

connective weights and membership functions of the FNNMFC. The output of the FNNMFC is the adaptive control signal, $U_{FNNMFC} = \delta i_{qs}^{r*}$.

$$e_\theta^{mf} = (\theta_r^{mf} - \theta_r) \tag{14}$$

$$\dot{\theta}_r = k_\theta d\theta_r / dt \tag{15}$$

3.1 Sliding-Mode Position Controller (SMC)

The structure of the sliding-mode control of the PMSM servo drive system is shown in Fig. 2. Rewriting the mechanical equation (8) at no-load and at nominal PMSM parameters will yield:

$$\ddot{\theta}_r(t) = A_m\dot{\theta}_r(t) + B_m.U(t) \tag{16}$$

While by considering the dynamics in (8) with parameter variations, disturbance load and unpredictable uncertainties will give:

$$\begin{aligned}\ddot{\theta}_r(t) = {} & (A_{mn} + \Delta A_m)\dot{\theta}_r(t) + (B_{mn} + \Delta B_m).U(t) \\ & + (D_{mn} + \Delta D_m).T_L\end{aligned} \tag{17}$$

$$\ddot{\theta}_r(t) = A_{mn}\dot{\theta}_r(t) + B_{mn}.U(t) + L(t) \tag{18}$$

Where ΔA_m, ΔB_m and ΔD_m are the uncertainties due to mechanical parameters J_m and β_m, and $L(t)$ is the lumped parameter uncertainty and is defined as:

$$L(t) = \Delta A_m\dot{\theta}_r(t) + \Delta B_m.U(t) + (D_{mn} + \Delta D_m)T_L \tag{19}$$

The bound of the lumped parameter uncertainty is assumed to be $|L(t)| \le K_{\theta S}$. The objective is to design a control law so that the rotor position of the PMSM can track any desired command. To achieve this control objective, we can define the error function $e_\theta(t) = (\theta_r(t) - \theta_r^*(t))$. The sliding surface can be defined as a proportional plus integral plus derivative (PID) performance measure and given by the following.

$$S(t) = K_{ps}e_\theta(t) + K_{ds}\dot{e}_\theta(t) + K_{is}\int_0^t e_\theta(\tau)d\tau \tag{20}$$

Where the positive constants K_{ps}, K_{ds} and K_{is} are designed based on the desired drive system dynamics such as rise time, overshoot and settling time. Rewriting (20), the sliding surface is given by:

$$S(t) = K_{ds}\left(K_{pds}e_\theta(t) + \dot{e}_\theta(t) + K_{ids}\int_0^t e_\theta(\tau)d\tau\right) \tag{21}$$

Differentiating $S(t)$ with respect to time and using the error position function $e_\theta(t) = (\theta_r(t) - \theta_r^*(t))$ will give:

$$\dot{S}(t) = K_{ds}\left(\ddot{\theta}_r(t) - \ddot{\theta}_r^*(t) + K_{pds}\dot{e}_\theta(t) + K_{ids}e_\theta(t)\right) \tag{22}$$

Inserting (18) into (22) will yield:

$$\begin{aligned}\dot{S}(t) = K_{ds}\big(& A_m\dot{\theta}_r(t) + B_mU_{SMC}(t) + L(t) - \ddot{\theta}_r^*(t) \\ & + K_{pds}\dot{e}_\theta(t) + K_{ids}e_\theta(t)\big)\end{aligned} \tag{23}$$

The tracking problem is to find a control law $U_{SMC}(t)$ so that the rotor position, θ_r, remaining on the sliding surface, $S(t)$, for all $t>0$. In the design of the sliding-mode control system, the ideal equivalent control law, which determines the dynamics of the drive system on the switching surface, is derived. The ideal equivalent control law is derived from $\dot{S}(t) = 0$. Applying this equality to (23) will provide:

$$\begin{aligned}&\ddot{\theta}_r^*(t) - A_{mn}\dot{\theta}_r(t) - B_{mn}U_{SMC}(t) - L(t) \\ &- K_{pds}\dot{e}_\theta(t) - K_{ids}e_\theta(t) = 0\end{aligned} \tag{24}$$

Where $K_{pds}=K_{ps}/K_{ds}$ and $K_{ids}=K_{is}/K_{ds}$ are positive constants.

From (24) and the lumped parameter uncertainty condition $|L(t)| \le K_{\theta S}$, the sliding-mode control objective is given by:

$$\begin{aligned}U_{SMC}(t) = i_{qs}^{r*} = {} & B_{mn}^{-1}[(\ddot{\theta}_r^*(t) - K_{pds}\dot{e}_\theta(t) \\ & - K_{ids}e_\theta(t)) - A_{mn}\dot{\theta}_r(t) - K_{\theta S}\,\mathrm{sgn}(S(t))]\end{aligned} \tag{25}$$

The first term in (25) describes the desired system performance, the second term is a torque estimator which is able to compensate for the nonlinear effect in the PMSM model, while the third term keeps the PMSM servo drive system dynamics on the sliding surface, $S(t)=0$

for the duration of the experiment.

The main advantage of the sliding-mode control is its insensitivity to parameter variations and external load disturbance in the switching surface. To keep the trajectory in the sliding surface, the selection of the control gain , $K_{\delta s}$, is very important due to its significant effect on the magnitude of the lumped parameter uncertainties of the PMSM servo drive system and hence its performance. The incorrect selection of this control gain will yield to the deviation from the sliding surface and cause chattering phenomena. To solve this problem an adaptive control signal, $U_{FNNMFC} = \delta i_{qs}^{r*}$, is generated to compensate for the error in the control effort of the sliding-mode position controller, $U_{SMC} = i_{qs}^{r*}$. Therefore, an FNNMFC is augmented to the sliding-mode position controller to preserve the desired tracking response under parameter variations (uncertainties) and external load disturbances. The following section includes the design of the FNNMFC.

3.2 Fuzzy – Neural – Network Model Following Controller

The online trained FNNMFC for a high-performance PMSM servo drive system integrates the ideas of the fuzzy logic controller and neural network structure into an intelligent control system. An ANN-based structure is introduced for the fuzzy logic control.

The nodes in the hidden layers perform as membership functions and fuzzy rules. The proposed FNNMFC is constructed from the fuzzy IF–THEN rules, which are based on a simple knowledge concerning the PMSM servo drive system. A learning algorithm is then used to update the parameters of the FNNMFC. The supervised gradient decent method, which uses a delta adaptation law, is utilized to train the proposed controller on-line. The proposed FNNMFC observes the behavior of the PMSM drive system and compares the actual performance to a desired reference model performance. The learning algorithm modifies the parameters of the FNNMFC based on the model-following error to match the desired reference model response [17].

(A) Architecture of the FNNMFC: The architecture of the proposed four-layers FNNMFC is shown in Fig. 3.

Nodes in the input layer represent input linguistic variables. Nodes in the membership layer act as the membership functions. All the nodes in the rule layer for a fuzzy rule base. In the proposed FNNMFC, which includes four-layers, an input layer (*i* layer), a membership layer (*j* layer), a rule layer (*k* layer) and an output layer (*o* layer) are two, six, nine and one respectively.

The nodes in layer 1 transmit the input signals to the next layer. Each node corresponds to one input variable. The input variables are the error signal, e_θ^{mf}, and the rate of change of the rotor position (speed), $K_\theta \dot{\theta}_r = K_\theta \omega_r$. In the following section, the signal propagation and the basic function in each layer are given as follows.

For every node *i* in the input layer, the input and the output of the network can be represented as:

For every node *i* in the input layer, the input and the output of the network can be represented as:

$$net_i^1 = x_i^1 \tag{26}$$

$$y_i^1 = f_i^1(net_i^1) = net_i^1 \qquad i = 1,2 \tag{27}$$

$$x_1^1 = e_\theta^{mf}(t) \quad \text{and} \quad x_2^1 = K_\theta \dot{\theta}_r(t) \tag{28}$$

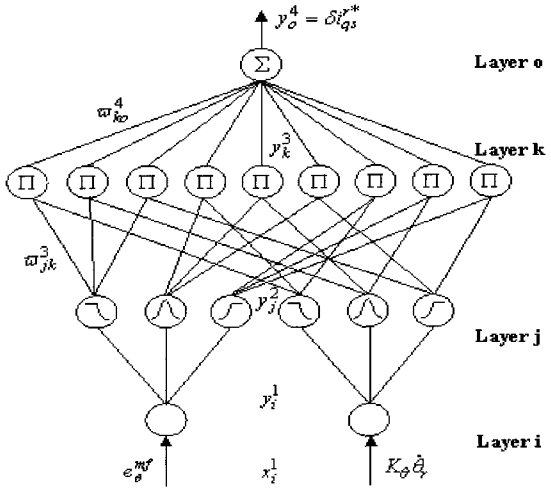

Fig. 3 Architecture of the FNNMFC

The nodes in layer 2 act as membership functions to express the input/output fuzzy linguistic variables. The Gaussian activation function is used to represent the membership function. For the *j*th node

$$net_j^2 = -\frac{(x_i^2 - \mu_{ij})^2}{(\sigma_{ij})^2} \tag{29}$$

$$y_j^2 = f_j^2(net_j^2) = \exp(net_j^2) \qquad j = 1,\ldots\ldots..,n \tag{30}$$

where μ_{ij} and σ_{ij} are the mean and the standard deviation of the Gaussian function in the jth term of the ith input linguistic variable x_i^2 to the node of layer 2 (membership layer) and n is the total number of the linguistic variables with respect to the input nodes. The weights between the input and membership layer are assumed to be in unity.

Each node in layer 3 (rule layer) is denoted by $\prod$ which multiplies the incoming signal and outputs the result of the product. Consequently, each node of this layer is a rule node that represents one fuzzy control rule. The links of layer 3 define the preconditions and the out come of the rule nodes respectively. For the kth nodes:

$$net_k^3 = \prod_j \varpi_{jk}^3 x_j^3 \tag{31}$$

$$y_k^3 = f_k^3(net_k^3) = net_k^3 \qquad k = 1,\ldots\ldots..,l \tag{32}$$

where x_j^3 represents the jth input to the node of the layer 3 (rule layer) and ϖ_{jk}^3 are the weights between the membership layer (layer 2) and the rule layer (layer 3). These weights are also assumed to be in unity; $l = (n/i)^i$ is the number of rules with complete rule connection if each input node has the same linguistic variables.

Layer 4 is the output layer and acts as a defuzzifier. The single node o in the output layer is denoted by Σ, which computes the overall output as the summation of all incoming signals to obtain the final inferred results.

$$net_o^4 = \sum_k \varpi_{ko}^4 x_k^4 \tag{33}$$

$$y_o^4 = f_o^4(net_o^4) = \left| net_o^4 \right| \qquad o = 1 \tag{34}$$

where the connecting weight ϖ_{ko}^4 is the output action strength of the oth output associated with the kth rule, x_k^4 represents the kth input to the node of output layer and $y_o^4 = U_{FNNMFC}$.

$$U_{FNNMFC}(t) = \delta i_{qs}^{r*}(t) \tag{35}$$

(B) On-Line Training Signal Analysis for FNNMFC: The selection of parameters for the weights and membership functions has a considerable effect on the network performance. If unsuitable values are specified for the weights and membership functions, the network will converge at a low speed. Therefore, an on-line parameter training methodology is used in order to train the FNNMFC effectively, which is derived using the gradient descent method. The connecting weights between rule layer and output layer are adjusted on line in addition to the weights and the membership functions. The essential part of the learning algorithm for an FNNMFC concerns how to obtain a gradient vector in which each element in the learning algorithm is defined as the derivative of the energy function with respect to a parameter of the network using the chain rule. Since the gradient vector is calculated in the direction opposite to the flow of the output of each node [17], the method is generally referred to as the back-propagation learning rule. To describe the on-line learning algorithm of the FNNMFC using the supervised gradient descent method, the energy function is chosen as:

$$E_\theta = \frac{1}{2}(\theta_r^{mf} - \theta_r)^2 = \frac{1}{2}(e_\theta^{mf})^2 \tag{36}$$

The learning algorithm based on the back-propagation method is described as follows.

In the output layer (layer 4), the error term to be propagated is calculated as:

$$\begin{aligned} \delta_o^4 &= -\frac{\partial E_\theta}{\partial net_o^4} = -\frac{\partial E_\theta}{\partial y_o^4}\cdot\frac{\partial y_o^4}{\partial net_o^4} \\ &= -\frac{\partial E_\theta}{\partial e_\theta^{mf}}\cdot\frac{\partial e_\theta^{mf}}{\partial net_o^4} = -\frac{\partial E_\theta}{\partial e_\theta^{mf}}\cdot\frac{\partial e_\theta^{mf}}{\partial \theta_r}\cdot\frac{\partial \theta_r}{\partial net_o^4} \end{aligned} \tag{37}$$

The weight is updated by the amount:

$$\begin{aligned} \Delta\varpi_{ko}^4 &= -\eta_\omega \frac{\partial E_\theta}{\partial \varpi_{ko}^4} \\ &= \left[-\eta_\omega \frac{\partial E_\theta}{\partial y_o^4}\cdot\frac{\partial y_o^4}{\partial net_o^4}\right]\cdot\frac{\partial net_o^4}{\partial \varpi_{ko}^4} = \eta_\omega \delta_o^4 x_k^4 \end{aligned} \tag{38}$$

Where η_ω is the learning rate parameter of the connecting weights of the FNNMFC. The weights of the output layer (layer 4) are updated according to the following equation.

$$\varpi_{ko}^4(N+1)=\varpi_{ko}^4(N)+\Delta\varpi_{ko}^4=\varpi_{ko}^4(N)+\eta_\omega\delta_o^4 x_k^4 \tag{39}$$

Where N denotes the number of iterations.

In rule layer (layer 3), only the error term needs to be computed and propagated because the weights in this layer are in unity.

$$\begin{aligned}\delta_k^3 &= -\frac{\partial E_\theta}{\partial net_k^3}\\ &=\left(-\frac{\partial E_\theta}{\partial y_o^4}\cdot\frac{\partial y_o^4}{\partial net_o^4}\right)\left(\frac{\partial net_o^4}{\partial y_k^3}\cdot\frac{\partial y_k^3}{\partial net_k^3}\right)=\delta_o^4\varpi_{ko}^4\end{aligned} \tag{40}$$

In the membership layer (layer 2), the multiplication operation is done. The error term is calculated as follows:

$$\begin{aligned}\delta_j^2 &= -\frac{\partial E_\theta}{\partial net_j^2}=\left(-\frac{\partial E_\theta}{\partial y_o^4}\cdot\frac{\partial y_o^4}{\partial net_o^4}\cdot\frac{\partial net_o^4}{\partial y_k^3}\cdot\frac{\partial y_k^3}{\partial net_k^3}\right)\\ &\cdot\left(\frac{\partial net_k^3}{\partial y_j^2}\cdot\frac{\partial y_j^2}{\partial net_j^2}\right)=\sum_k\delta_k^3 y_k^3\end{aligned} \tag{41}$$

The update law of the mean of the Gaussian function is given by:

$$\begin{aligned}\Delta\mu_{ij} &= -\eta_\mu\frac{\partial E_\theta}{\partial\mu_{ij}}=\left[-\eta_\mu\frac{\partial E_\theta}{\partial y_j^2}\cdot\frac{\partial y_j^2}{\partial net_j^2}\cdot\frac{\partial net_j^2}{\partial\mu_{ij}}\right]\\ &=\eta_\mu\delta_j^2\frac{2\left(x_i^2-\mu_{ij}\right)^2}{(\sigma_{ij})^2}\end{aligned} \tag{42}$$

The update law of the standard deviation of the Gaussian function is given by:

$$\begin{aligned}\Delta\sigma_{ij} &= -\eta_\sigma\frac{\partial E_\theta}{\partial\mu_{ij}}=\left[-\eta_\mu\frac{\partial E_\theta}{\partial y_j^2}\cdot\frac{\partial y_j^2}{\partial net_j^2}\cdot\frac{\partial net_j^2}{\partial\sigma_{ij}}\right]\\ &=\eta_\sigma\delta_j^2\frac{2\left(x_i^2-\mu_{ij}\right)^2}{(\sigma_{ij})^2}\end{aligned} \tag{43}$$

Where η_μ and η_σ are the learning rate parameters of the mean and standard deviation of Gaussian functions respectively. The mean and standard deviation of the membership functions in this layer are updated as follows:

$$\mu_{ij}(N+1)=\mu_{ij}(N)+\Delta\mu_{ij} \tag{44}$$

$$\sigma_{ij}(N+1)=\sigma_{ij}(N)+\Delta\sigma_{ij} \tag{45}$$

To overcome the problem of uncertainties of the PMSM due to parameter variations and to increase the on-line learning rate of the network parameters, a control law is proposed as follows.

$$\delta_o^4=e_\theta^{mf}+K_\theta\dot{\theta}_r \tag{46}$$

4. Simulation Results

The efficacy of the proposed scheme for the PMSM servo drive system shown in Fig. 1 is verified by computer simulations based on MATLAB/SIMULINK [18]-[19].

4.1 Dynamic Performance at Nominal Parameters

The simulations results of the PMSM servo drive systems are presented to verify the feasibility of the proposed control scheme under various operating conditions. The dynamic performance of the drive system due to reference model of 2π rad under subsequent loading of 0-3.6 N.m is predicted as illustrated in Fig. 4. The disturbance rejection capabilities have been checked when a load of 3.6 N.m is applied to the shaft at t = 1.5 s and removed after a period of 1.625 s. The simulation results of the proposed sliding-mode position controller shown in Fig. 4 include the command and actual responses for the rotor position, the rotor speed, d-q axes stator currents in the rotating reference frames and the sliding surface $S(t)$ for both SMC and ISMC controllers at Case 1. These Figures clearly illustrate favorable tracking responses and robust characteristics in command tracking and load regulation performance are realized for both controllers. The sliding motion characteristics without reaching phase are obvious by determining the sliding-surface shown in Fig. 4.

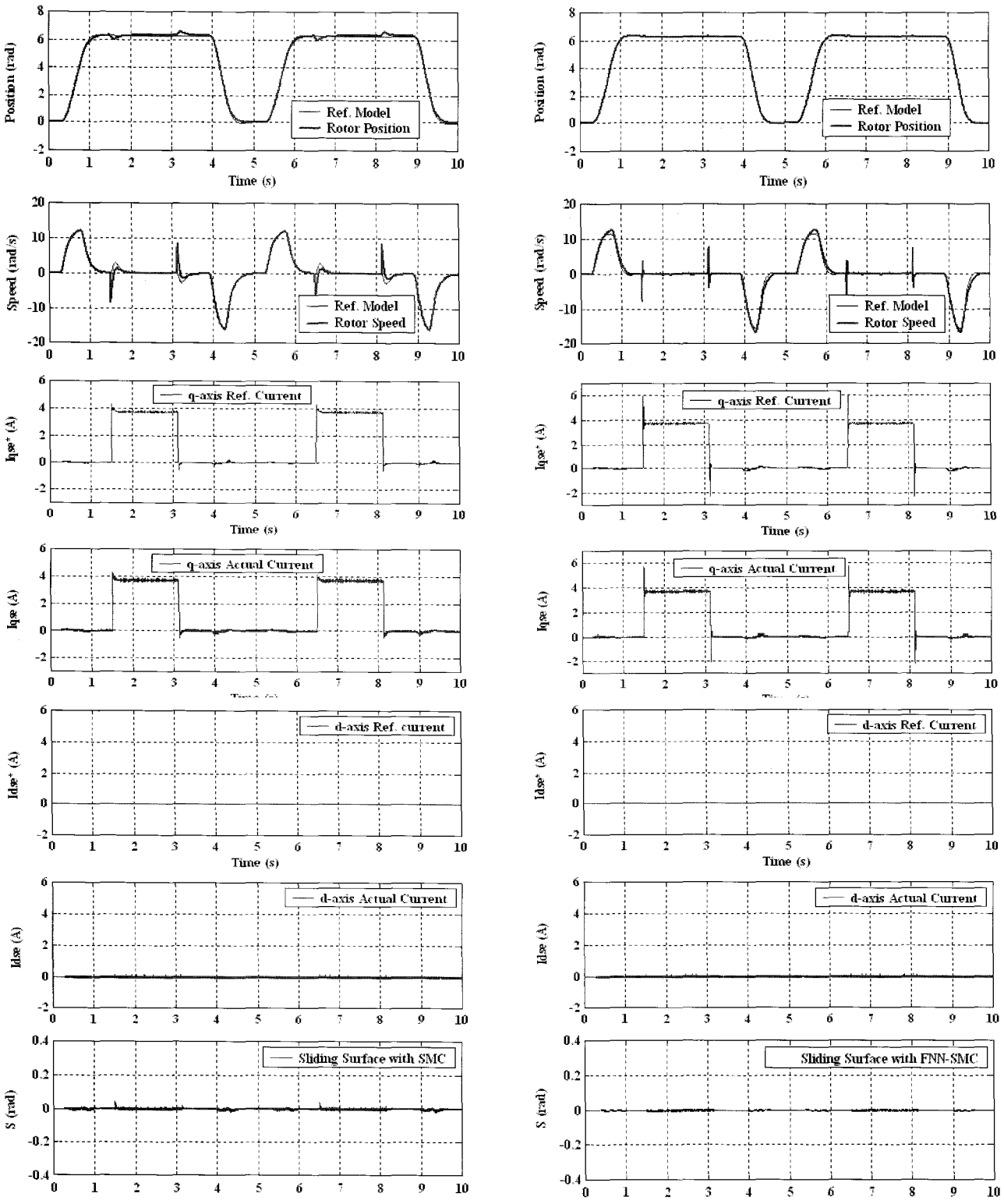

(a) Dynamic response using SMC (b) Dynamic response using ISMC

Fig. 4 Dynamic response for a reference model of 2π rad and loading of 3.6 N.m of the servo drive system for both position controllers

Improvement of the control performance by augmenting the proposed FNNMFC to the SMC shown in Fig. 2 can be observed from the obtained results in command tracking and load regulation characteristics. The model-following response and the model-following error (MFE) for both position controllers are given in Fig. 5. Also, it is evident that from Fig. 5 an obvious model-following error (MFE) due to the SMC reaches to 0.15 rad while the MFE due to ISMC is about 0.05 rad. The results obtained in Fig. 6 illustrate the model-following response and load regulation performance for both position controllers. It is clear from this Figure that a good model-following response is granted using the SMC with FNNMFC. It is clear from this Figure that the proposed ISMC with FNNMFC provides a rapid and accurate response for the reference model. Also, the proposed controller quickly returns the rotor position to the reference model under full load condition with a recovery time of 0.05s and a maximum dip of 0.053 rad while the SMC provides a slow response for the reference model under full load condition with a long recovery time of about 0.5s and a large dipping in the rotor position of about of 0.28 rad. Therefore, the proposed ISMC provides a good model-following response, tracking characteristics and load regulation performance.

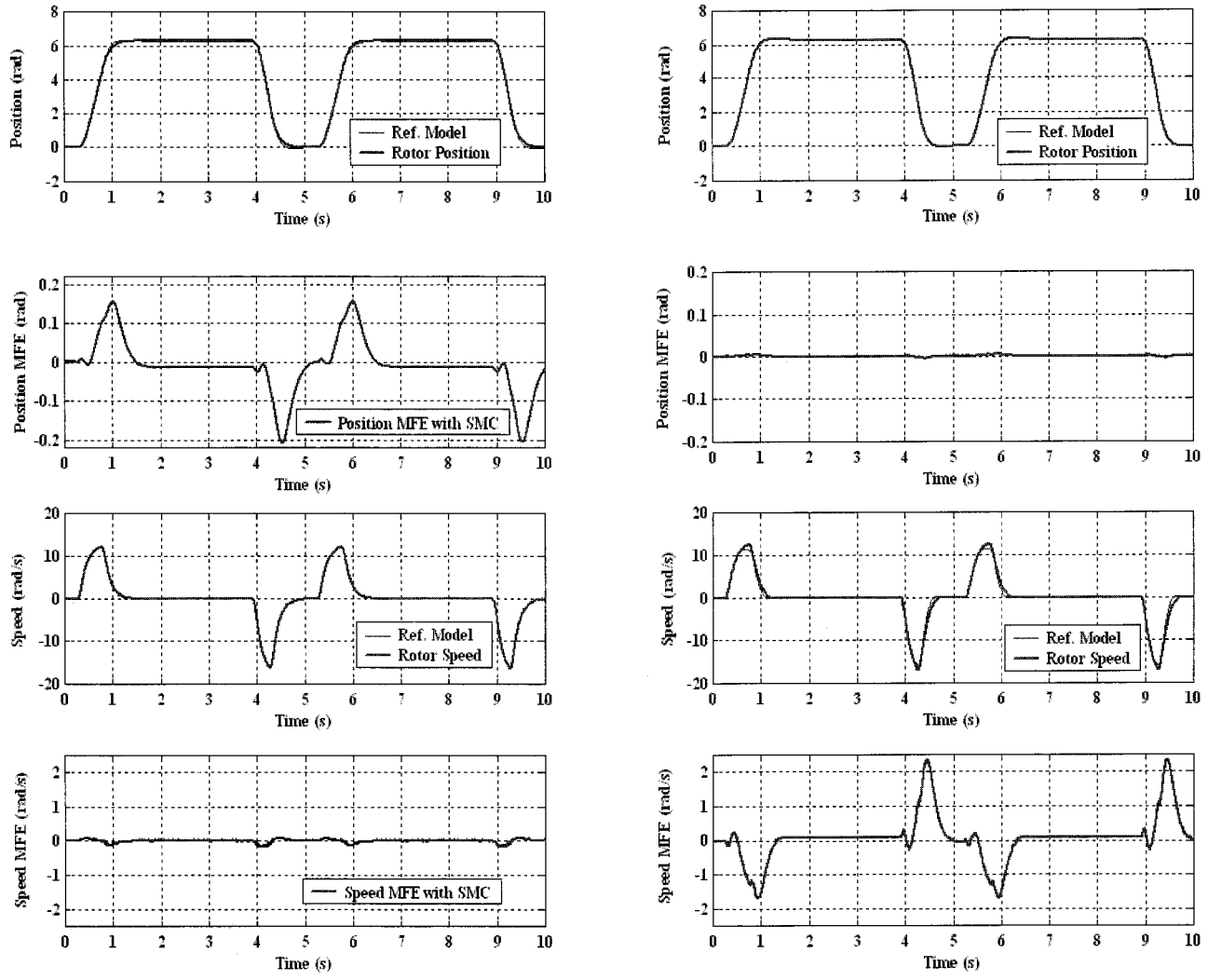

(a) Using SMC (b) Using ISMC

Fig. 5 The Position and speed tracking response and model-following error (MFE) responses of the servo drive system at no-load for both position controllers

[10] Fayez F. M. El-Sousy, "A Vector-Controlled PMSM Drive with a Continually On-Line Learning Hybrid Neural-Network Model-Following Speed Controller," *The Korean Institute of Power Electronics (KIPE), Journal of Power Electronics (JPE)*, Vol. 5, No. 2, pp. 197-210, April 2005.

[11] Fayez F. M. El-Sousy, "Intelligent Model-Following Position Control for PMSM Servo Drives," *6th WSEAS International Conference on Neural Networks, Lisbon, Portugal*, pp. 230-238, June 16-18, 2005.

[12] Faa-Jeng Lin, and Chih-Hong Lin, "A Permanent-Magnet Synchronous Motor Servo Drive Using Self-Constructing Fuzzy Neural Network Controller," *IEEE Trans. on Energy Conversion*, Vol. 19, No. 1, pp. 66–72, March 2004.

[13] Faa-Jeng Lin, Chih-Hong Lin, and Po-Hung Shen, "Self-Constructing Fuzzy Neural Network Speed Controller for Permanent-Magnet Synchronous Motor Drive," *IEEE Trans. on fuzzy systems*, Vol. 9, No. 5, pp. 751–759, October 2001.

[14] F. J. Lin, W. J. Huang, and R. J. Wai, "A supervisory fuzzy neural network control system for tracking periodic inputs," *IEEE Trans. Fuzzy Syst.*, Vol. 7, pp. 41–52, Feb. 1999.

[15] Y. S. Lu and J. S. Chen, "A self-organizing fuzzy sliding-mode controller design for a class of nonlinear servo systems," *IEEE Trans. Indust. Electron.*, Vol. 41, pp. 492–502, Oct. 1994.

[16] F.-J. Lin and S. L. Chiu, "Adaptive fuzzy sliding-mode control for PM synchronous servo-motor drives," *IEE Proc. Control Theory Application*, Vol. 145, No. 1, pp. 63-72, 1998.

[17] Y.C Chen and C.C Teng, "A model reference control structure using a fuzzy neural network," *IEEE Transaction on Fuzzy Sets and Systems.*, Vol. 73, pp. 291-312, 1995.

[18] *Matlab Simulink User Guide*, The Math Work Inc., 1997.

[19] C. M. Ong, *Dynamic Simulation of Electric Machinery Using Matlab and Simulink*, Printice Hall, 1998.

Fayez F. M. El-Sousy was born in Gahrbia Prefecture, Egypt in 1965. He received the B.Sc. degree in Electrical Power and Machines Engineering from Menoufia University, Egypt in 1988, the M.Sc. degree in Electrical Power and Machines Engineering from Cairo University, Egypt in 1994 and the Ph.D degree in Electrical Power and Machines Engineering from Cairo University, Egypt in 2000. Since 1990, he has been with the Department of Power Electronics and Energy Conversion at the Electronics Research Institute (ERI) where he is currently an Associate Professor. From April 2004 to October 2004 he was a Post Doctoral visiting researcher at Kyushu University, Graduate School of Information Science and Electrical Engineering, Energy Conversion Laboratory, Japan. His research interests are in the areas of modeling and control of IM, PMSM, LIM and PMLSM drives, intelligent control, optimal control and power electronics. Dr. El-Sousy is currently interested in the robust control of the linear motor Maglev drive system.